OVERVIEW OF THE NASA ENTRY, DESCENT AND LANDING SYSTEMS ANALYSIS EXPLORATION FEED-FORWARD STUDY

Alicia D. Cianciolo[(1)], Thomas A. Zang[(1)], Ronald R. Sostaric[(2)], M. Kathy Mcguire[(3)]

[(1)]NASA Langley Research Center, MS 489, Hampton VA USA 23681
Email:Alicia.M.DwyerCianciolo@nasa.gov, Thomas.A.Zang@nasa.gov
[(2)]NASA Johnson Space Center, 2101 NASA Parkway, Mail Code EG5, Houston TX USA 77058
Email:Ronald.R.Sostaric@nasa.gov
[(3)]NASA Ames Research Center, MS 258-1, Moffett Field, CA USA 94035, Email:Kathy.Mcguire@nasa.gov

ABSTRACT

Technology required to land large payloads (20 to 50 mt) on Mars remains elusive. In an effort to identify the most viable investment path, NASA and others have been studying various concepts. One such study, the Entry, Descent and Landing Systems Analysis (EDLSA) Study [1] identified three potential options: the rigid aeroshell, the inflatable aeroshell and supersonic retropropulsion (SRP). In an effort to drive out additional levels of design detail, a smaller demonstrator, or exploration feed-forward (EFF), robotic mission was devised that utilized two of the three (inflatable aeroshell and SRP) high potential technologies in a configuration to demonstrate landing a two to four metric ton payload on Mars.

This paper presents and overview of the maximum landed mass, inflatable aeroshell controllability and sensor suite capability assessments of the selected technologies and recommends specific technology areas for additional work.

1. OBJECECTIVES

The objectives of this study were to use 3 and 6 degree of freedom (DOF) Program to Optimize Simulated Trajectories (POST2) [2] simulations to characterize the performance of various aspects of the system design to inform work in other areas of concurrent or planned study at NASA. For example, a main objective of the study was to determine the maximum payload mass (to Mars touchdown) capability of a Delta IV-H launch vehicle, given the spacecraft launch mass constraint of 7.2 t and assuming the 2024 Mars opportunity. Few detailed payload definitions exist. This objective was to identify the capability of this type of system while demonstrating technologies that could eventually be used on much larger scales.

A second objective was to characterize the performance required of the SRP system. SRP has been identified on the critical path to land humans on Mars. Studies are underway to determine the path to maturity. Results from this study provided information on intermediate system requirements.

A third major objective was to use the high fidelity entry simulation to characterize an Autonomous Landing and Hazard Avoidance Technology (ALHAT) like sensor suite for Mars. The 6 DOF simulation provided Mars specific performance information for sensor operational ranges required to the ALHAT team.

A final objective was to assess the controllability of the inflatable aeroshell also called a Hypersonic Inflatable Aerodynamic Decelerator (HIAD). HIADs are a new technology and little is know about the ability to control large inflatable devises in a range of aerodynamic conditions.

The following sections summarize the analysis performed to meet the stated objectives, the study results passed along to other working groups and recommendations for future investment.

2. LANDED MASS ASSESSMENT

The feed-forward vehicle consisted of three major mass components: the payload, the inflatable aeroshell and the descent landing vehicle which included SRP. A parameterized mathematical mass model represented each component as a function of vehicle dimension and key environmental parameters (i.e. dynamic pressure and total heat load). Details of the parameterization can be found elsewhere [3,4] but the primary purpose of the model was to facilitate rapid design optimization and trade studies. A description of the system and the major mass components is provided below.

2.1 Payload

The candidate payload for this study was a small Movable Fission Power System (MFPS) [5] shown in Fig 1. The power plant mass is 1615 kg, and the mass for power management and distribution system is 415 kg, yielding a target landed payload of approximately 2

t. There are two options for payload surface mobility, and though neither was included in the current study, there appears to be sufficient landed payload capability to include them with the MFPS on a single lander.

Analysis was done to determine the payload's mass properties as defined in [5]. The values were used in the HIAD controllability and ALHAT 6DOF analyses. However, mass modeling simulation considered only 3DOF trajectories to determine maximum landed mass and did not rescale the payload mass properties according to landed payload capability greater than 2 t. The impact of the change in the mass properties to accommodate larger vehicle was not evaluated. However, the controller was designed to generated pure accelerations and did not define thruster size, location or orientation. Therefore the 6DOF analysis could be performed independent of the payload mass properties.

It was also recognized that the payload configuration presented in [5] might not be optimal for the entry configuration (HIAD + SRP) selected for the study. Options to shorten the payload were considered but the team elected to use the payload as defined and impose constraints on the diameter of the HIAD (minimum of 8 m) and the angle of attack (>17 deg) to mitigate flow impingement issues that may result from the long payload.

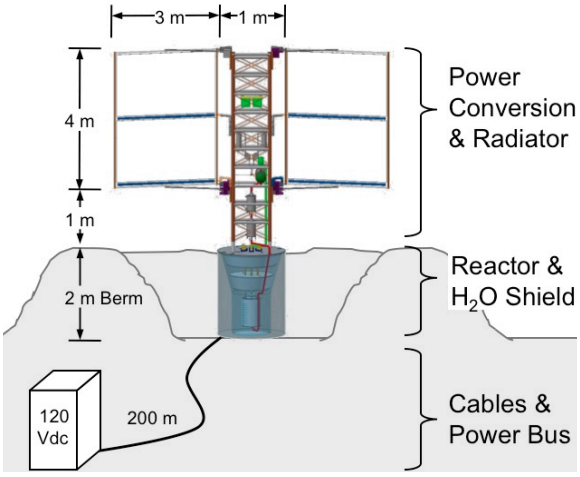

Fig. 1. Movable Fission Power System Concept [3]

2.2 Inflatable Aeroshell

The inflatable aeroshell or HIAD consists of two main components contributing to the system mass: the structure and the thermal protection system (TPS). Each is described below.

Structure

The HIAD structure model is a 65° sphere cone aeroshell that includes an inflatable decelerator, separation mechanism, payload adapter, and a 4 m rigid spherical aeroshell. The mass of the inflatable decelerator is based on the models developed by NASA in the 1960's and 1970's. A detailed description can be found in [1] and [6] and is shown (inflatable in yellow and aeroshell in beige) attached to the payload in Fig. 2.

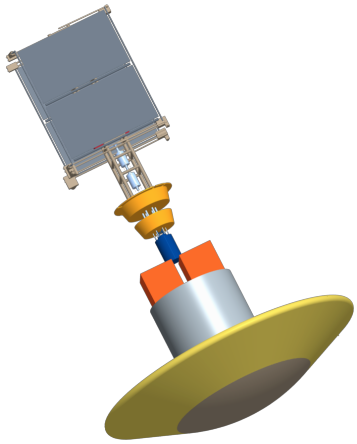

Fig. 2. HIAD Vehicle Configuration with ablator TPS and attached to the payload and descent stage

TPS

The thermal protection system (TPS) is one of the key components of HIAD aeroshells; it protects the inflatable decelerator from the extreme thermal environment during the aerocapture and entry phases. The HIAD TPS must be lightweight, suitable for efficient packaging and be capable of performing its function upon deployment after being stowed for periods of up to 6 months. Ablator and insulator concepts are currently two primary candidates for the HIAD TPS. The ablator mass model used in this study was developed at NASA Ames Research Center, and it was based on SIRCA-flex (flexible Q-felt plus silicone matrix) and PICA-flex (flexible Q-felt plus phenolic matrix)) concepts [7,8]. The insulator mass model was developed at NASA Langley Research Center, and it was based on a multilayer concept with an outer fabric (Nextel 440), an insulator (Pyrogel 3350), and a laminated gas barrier (Kapton-Kevlar-Kapton layer). The model, based on the IRVE 3 and 4 concepts, does have manufacturability, packaging and development maturity.

The ablator TPS concept has a higher areal density than that of the insulator, but can operate in environments with higher heat rates (up to 115 W/cm^2 for SIRCA-flex and up to 450 W/cm^2 for PICA-flex [8]). Insulators are currently limited to peak heat rates of ~60 W/cm^2. The optimal diameter for ablator and insulator HIADs are different: ablators tend to be more mass efficient for smaller diameter HIADs, while the

insulators are more mass efficient for larger diameters HIADs.

2.3 Descent Stage

The descent stage mass model, which includes the supersonic retropropulsion and associated hardware, was sized using The Exploration Architecture Model for IN-space and Earth-to-orbit (EXAMINE) [9] modeling framework. The primary descent stage structure is a 2.6 m diameter aluminum-lithium (Al-Li) cylinder that supports the tank system and payload. Thrust structure mass is based on a historical fit accounting for stage diameter, the number of engines and the thrust load. Secondary structure mass is 5% of the primary plus thrust structure masses. Landing gear mass is 2.5% of the landed mass on Mars. Multilayer insulation (MLI) is 5 cm thick (39.4 kg/m3) covering the exterior structure, providing thermal control of the spacecraft. During trans-Mars coast, a 3-junction gallium-arsenide photovoltaic array that provides 0.5 kilowatts (kW) of power for the EFF spacecraft. During entry and landing, two lithium-ion batteries each provide 1 kW for 2 hours of operation with 100% depth of discharge. Power is managed and distributed with a 115 volt alternating current system sized to handle 1 kW peak power at 90% efficiency. Waste heat (up to 1 kW) is collected from coldplates using an ammonia fluid loop and rejected using a body-mounted radiator. Avionics, including command, control and data handling, communication, guidance, navigation and control (GN&C), and instrumentation, are derived from MSL.

Four pump-fed NTO/MMH engines are used for the main supersonic retropropulsion system and operate at 856 psia chamber pressure and a mixture ratio of 2.05. The engines are derived from the RS-72 engine in development at Rocketdyne that delivers 12,000 pounds of thrust per engine.

2.4 Entry Configurations

The three major components were then combined in various EFF configurations and entry conditions. The 3DOF simulation was used to determine the combination that delivered the maximum payload. Details of the simulation can be found in [4]. All configurations considered are shown in Fig. 3.

Combination 1: Ablator vs Insulator TPS
The baseline case considered a dual HIAD option, which used one HIAD for the aerocapture into a 500 km sol orbit then jettisoned the HIAD prior to deploying a second for entry. The difference in the two cases was only the choice of TPS material used. Because the ablator material could accomidate a higher heat load environment, the diameter was reduced (from 14 m to 8 m) resulting in ~11% increase in payload mass. See EFF-1 configuration in Fig. 3 and results in Table 1.

Combination 2: Dual vs Single HIAD
The second trade evaluated the potential mass savings over mission complexity. The dual HIAD option eliminated the complexity of HIAD reinflation and risk of material degradation from the first heat pulse of a single HIAD system. However, the mass required for a second HIAD system did reduce the payload mass capability of the systems using the same TPS. EFF-2 demonstrated a single HIAD configuration for both types of TPS. The resulting payload mass for the single HIAD was higher than the dual HIAD (EFF-1) by about 10% and the difference between the single HIAD ablator vs insulator payload was again approximately 10%.

Combination 3: Direct Entry vs. Aerocapture
The trade of eliminating the aerocapture HIAD for a single HIAD which enters at a higher velocity (7.2 km/s vs 3.8 km/s from aerocaptured orbit) resulted in even higher payload capability compared to Combination 1 or 2 due to the fact no aerocapture system was needed and that the diameter of the entry HIAD using ablator material was sufficient at 8 m but the HIAD using insulator needed to be increased in diameter from 14 to 16 m. However the delivered payload for both configurations was nearly the same. See EFF-3 in Fig 3 and Table 1.

Combination 4: Direct Entry speed of 7.3 vs 5.8 km/s
The velocities were selected to represent a "worse case" opportunity (2024) and a MSL type opportunity respectively. The lower entry velocity resulted in lower heating environment and thus reduced the mass of the entry HIADs for both TPS systems. This configuration yielded the highest payload mass of the configurations considered at nearly 3.5 mt. The difference between the TPS systems yielded only a 4% difference in payload mass. A redesign of the payload that allows for a smaller diameter entry HIAD would further increase the payload capability of the system. See EFF-4 in Fig. 3 and Table 1.

3. ALHAT SENSOR ASSESSMENT

The objective of the ALHAT sensor assessment was to develop a 6DOF entry simulation to determine the sensor performance ranges for an ALHAT-like system at Mars. The sensor suite included the ALHAT Extended Kalman filter (EKF), without TRN update capability and statistically-based IMU, startracker, altimeter and velocimeter models.

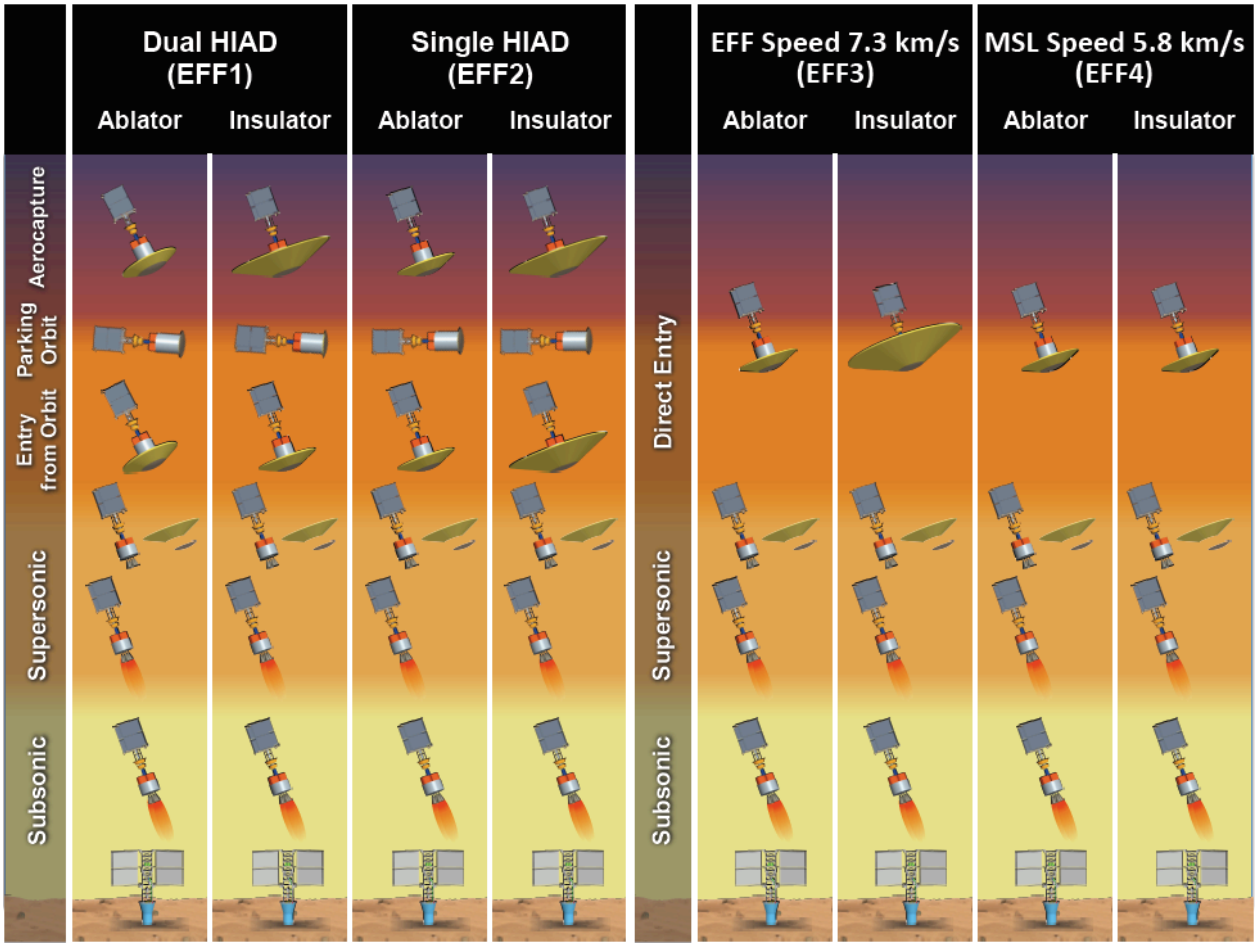

Figure 3. Exploration Feed Forward Concepts

Table 1. Mass and Environmental Results for Each Exploration Feed Forward Concept.

			EFF-1 Dual HIAD		EFF-2 Single HIAD			EFF-3 Direct Entry, 7.2 km/s		EFF-4 Direct Entry, 5.8 km/s	
	Units		Ablator	Insulator	Ablator	Insulator		Ablator	Insulator	Ablator	Insulator
Maximum Payload	kg	Aerocapture	**2627**	**2371**	**2881**	**2589**	Direct Entry	**3294**	**2953**	**3442**	**3584**
Diameter	m	Aerocapture	8	14	8	14	Direct Entry	8	16	8	8
Max Dynamic Pressure	Pa	Aerocapture	4259	1464	4259	1464	Direct Entry	5922	2017	5791	2781
Inflatable Mass	kg	Aerocapture	85	204			Direct Entry	113	395	111	60
Max Heat Rate	W/cm2	Aerocapture	108.7	44.5	108.6	44.5	Direct Entry	111	48	67	49
Heat Load	MJ/m2	Aerocapture	109	44	109	44	Direct Entry	80	26	41	51
TPS Mass	kg	Aerocapture	347	524			Direct Entry	367	685	304	183
Rigid Diameter	m	Aerocapture	4.3	4.3	4.3	4.3	Direct Entry	4.3	4.3	4.3	4.3
Rigid Heatshield Mass	kg	Aerocapture	91	91			Direct Entry	91	91	91	91
Payload Adaptor Mass	kg	Aerocapture	71	71			Direct Entry	71	71	71	71
Separation Mass	kg	Aerocapture	58	66			Direct Entry	59	76	58	53
Diameter	m	Entry	8	8	8	14					
Max Dynamic Pressure	Pa	Entry	1248	1147	1460	500					
Inflatable Mass	kg	Entry	40	38	85	204					
Max Heat Rate	W/cm2	Entry	5.0	4.5	5	2					
Heat Load	MJ/m2	Entry	14.8	15.1	17	8					
TPS Mass	kg	Entry	198	165	417	744					
Rigid Diameter	m	Entry	3.6	3.6							
Rigid Heatshield Mass	kg	Entry	64	64	91	91					
Payload Adaptor Mass	kg	Entry	64	61	71	71					
Separation Mass	kg	Entry	45	44	60	72					

The EFF simulation also ran the integrated GNC with sensors to evaluate SRP for Hazard Detection and Avoidance (HDA) and Terrain Relative Navigation (TRN). The EFF simulation included 6DOF entry with Apollo entry guidance and an LQR bank angle controller and 3DOF powered descent with Apollo powered descent guidance and a pseudo controller.

3.1 TRN and HDA Feasibility Test

The first step in evaluating TRN and HDA is to confirm that the viewing angle is compatible with the vehicle attitude.

TRN works over a wide range of altitude and velocity and is possible anytime the sensor is with in operating ranges and a high-quality map of the terrain is available. There are two basic forms of TRN; optical TRN, which uses optical cameras in the visible spectrum, and active TRN, which uses an altimeter, flash lidar, or other active sensor. Fundamentally, all that is needed is to ensure that this sensor has a view of the surface and that the navigation has a reasonable estimate of the vehicle's inertial position. Since the attitude profile during the first 60 sec prior to touchdown is well off of the vertical (see Fig. 4) it can reasonably be assumed that TRN measurements can be taken and that TRN is feasible.

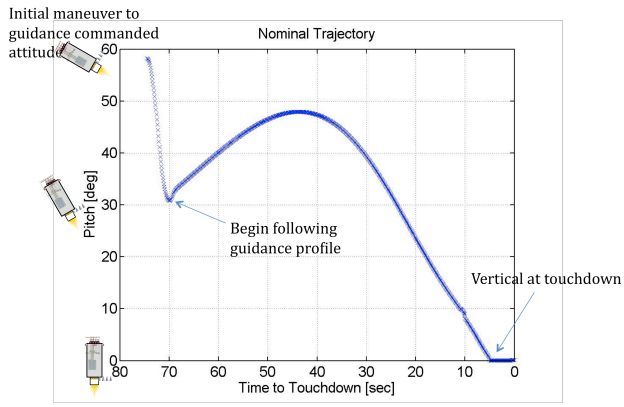

Fig. 4. Vehicle Pitch Profile During Powered Descent

Feasibility for HDA is more complex to demonstrate than for TRN. The flash lidar must scan the landing area, so it requires a line of sight to the landing area at the correct time during the descent. The lidar will be designed for optimum performance at a particular slant range from the landing site. The scan must occur at this distance to ensure that sufficient resolution is achieved and the full landing area can be scanned.

An initial analysis of the nominal trajectory shows that HDA is feasible for the nominal trajectory by looking out the back side of the vehicle (in the same direction in which TRN would occur) at an altitude of 1 km. However, in dispersed cases the look angle may be close to zero and the distribution may be both positive and negative at the time of the scan. This would require two sensors, one on each side of the vehicle. The trajectory can likely be redesigned such that all look angles are positive, for a minimal cost in additional propellant usage – and only would require one HDA sensor. Further investigation is needed before a conclusive determination can be made regarding HDA feasibility.

3.2 Navigation Performance

The ALHAT navigation filter used in the study is an EKF that provides estimates of the vehicle state (inertial position, inertial velocity and attitude quaternion). The EKF uses the Inertial Measurement Unit (IMU) for propagation while it receives updates (in the form of altimeter, startracker, velocimeter and TRN measurements) to improve state estimation. The ALHAT EKF initial performance and functionality was analyzed by running two Monte Carlo simulations, one with and one without TRN measurements. Since the delivery of the filter did not contain a TRN update capability, TRN measurements were mimicked using the simple propagator navigation filter for a comparison case. Details of the Monte Carlo assumptions can be found in [4].

At deorbit, or simulation initialization, initial inertial position navigation error was 3.5 km (99.87%-tile) and inertial velocity navigation error was 3.5 m/s (99.87%-tile). These errors are very conservative and may be adjusted with sensor measurement updates prior to deorbit. The resulting inertial navigation position error at entry was improved through propagation of the IMU updates to 3 km (99.87%-tile) and inertial velocity error was 3 m/s (99.87%-tile). The altimeter updates in the ALHAT EKF Monte Carlo began at engine ignition (nominally, 6 km altitude) and improve the altitude navigation error from 3.4 km (44% error) down to 11 m (1% error) (99.87%-tile), also improving inertial navigation position error from 4 km down to 2.8 km (99.87%-tile) at touchdown. The velocimeter updates in the ALHAT EKF Monte Carlo began at a 2 km altitude and improve relative velocity error from 3 m/s (1% error) down to 2 cm/s (0.01% error) (99.87%-tile), also improving inertial navigation velocity error from 5 m/s down to 17 cm/s (3-sigma). The range of fuel remaining at touchdown was 249.5 kg (0.13%-tile) to 870.5 kg (99.87%-tile). The results showed good initial ALHAT EKF performance. The range-to-target at touchdown, using the navigation updates and SRP, can get within 2.4 km (99.87%-tile) of the landing target. However, more improvement in navigation position error is needed to reduce the touchdown footprint.

The ALHAT EKF Monte Carlo (no TRN) was compared to an ideal TRN Monte Carlo where three TRN updates were mimicked as position navigation error reductions down to 85 m (conservative, based on ALHAT project analysis) during SRP. Results showed that inertial navigation position error was reduced from 4 km at engine ignition down to 125 m (99.87%-tile) at touchdown, compared to a reduction down to only 2.8 km (99.87%-tile) from the ALHAT Monte Carlo results. Improvement in navigation position error in form of TRN updates is needed to reduce the touchdown footprint

Additional performance numbers passed along to the ALHAT included TRN expected ranges to be between 2 and 7 km at velocities between Mach 0.5 to 1.7. The nominal HDA conditions resulted in activation below one km with a look angle of -14 deg and a path angle of 66 deg. The altimeter was activated at 6 km and the velocimeter at 2 km and 150 m/s.

4. SRP PERFORMANCE ASSESSMENT

An objective of the study was to characterize the system SRP requirements. The study, which assumed four engines with a specific impulse of 338s and a system thrust-to-weight of 3.7 Mars g's, yielded descent engine initiation between Mach 1.4 and 1.8 at an altitude between 3 and 8 km. This information was passed along to the EDL Technology Development Project.

5. HIAD CONTROLLABILITY ASSESSMENT

Identified as a light weight technology to enable large landed payloads at Mars, many concerns still exist for HIAD's including manufacturability, packaging, and degradation during cruise to Mars. Another concern is the ability to maneuver or control these large vehicles during atmospheric flight of aerocapture or entry.

To evaluate this, the 6DOF POST2 simulation was used to model only aerocapture into a 500 km circular orbit assuming a vehicle Lift to Drag (L/D) ratio of 0.25. The HIAD had an inflatable diameter of 14 m with a rigid aeroshell with a 4 m diameter and a ballistic coefficient of 33 kg/m2. Trajectories were constrained to a heat rate of 50 W/cm2 to accommodate insulative TPS. Trades were made using different guidance and control algorithms, initial orbit and L/D.

5.1 Guidance Algorithms

Four guidance algorithms were used in the assessment. First, the Hybrid Predictor-Corrector Aerocapture Scheme (HYPAS) has aerocapture study heritage dating back 10 years and has proven to be robust to a wide variety of L/D, ballistic coefficients, atmospheres, entry conditions, and target orbits. HYPAS targets a lifting vehicle through the atmosphere to a desired exit orbit apoapsis and inclination by using an analytically-derived guidance algorithm based on deceleration due to drag and altitude rate error feedback to determine the bank angle magnitude, and the inclination error to determine bank direction.

The Terminal Point Controller (TPC), closely related to the Apollo Earth Return entry guidance and the second guidance algorithm considered, is based on the Calculus of Variations, with boundary conditions derived for the aerocapture mission. It is robust and requires very little on-board code. A reference trajectory is defined for the aerocapture mission and that trajectory is used to develop sensitivities of the terminal point to changes in the lift vector at any point along the trajectory. These sensitivities are used to adjust the bank angle during flight to achieve the desired apoapsis at atmospheric exit. Lateral control is achieved by reversing the sign of the bank angle whenever the lateral error exceeds a variable-width deadband.

Next, the Numerical Predictor Corrector (NPC) guidance integrates a simplified set of the equations of motion and iterates the appropriate control parameter to meet the specified constraints. The NPC guidance determines the bank angle profiles and the required propulsion orientation during terminal descent to provide the proper landing conditions.

Finally, the Shape Integral (SI), the newest of the four, is based on an algebraic solution to the equations of motion in a plane. Normalized integral quantities, termed shape integrals, are calculated from a reference trajectory, providing the guidance gains. The velocity equation is first solved to determine the time-to-go. Then the altitude rate equation is solved for the appropriate scaling of a reference lift profile that is required to meet the targeted terminal conditions at atmospheric exit. Bank reversals are commanded to maintain a wedge angle, with respect to the target orbital plane, within set deadbands.

5.2 Controller Algorithms

Two control actuation schemes were considered for the EFF vehicle. The first is the 6DOF Bank Angle Controller performed using a Linear Quadratic Regulator (LQR) formulation. LQR provides a systematic approach to multi-input, multi-output control systems. The controller is based on aircraft equations of motion that have been decoupled into

longitudinal and lateral/directional subsets and linearized. Currently, it is assumed that pure torques about each vehicle axis are available at any level desired. The same controller structure is used for both the aerocapture and entry missions with different sets of gains.

The second was the 6DOF Center of Gravity (CG) Controller. It is actually a combination of CG control and a small RCS system to provide roll control. A single PID controller commanding a pure roll torque to drive the roll angle to zero provides roll control. In the vertical and horizontal channels, the guidance provides a commanded lift. Each of those commands is passed to a PID controller, which commands a payload position. The payload position command is passed to a second order actuator model, which moves the payload and the resultant CG is computed by the POST2 trajectory simulation. Forces to move the payload are assumed to be as large as necessary, but the actuator limits payload rates and accelerations.

5.3 Trade Results

As mentioned, trades were made using different guidance and control algorithms, initial orbit and L/D. All of the guidance algorithms were able to successfully aerocapture without violating the constraints using the bank controller. Issues arose with the use of the CG controller and that portion of the study remains incomplete. A complete set of results can be found in [10].

Minimum L/D

Because the results of the four guidances were comparable, one was selected to do further trade studies. The HYPAS guidance was used to determine the lowest feasible L/D for aerocapture. The results was that the L/D of 0.10 is still able to reach the target apoapsis, but inspection of the performance associated with individual lower L/D cases shows instances where the guidance is fully saturated. Guidance saturation occurs when the guidance must command maximum lift for the entire trajectory, leaving it no authority to fly out additional dispersions. To remedy this, the lateral corridor width is expanded for the lower L/D cases resulting in larger plane change maneuver delta-V. Therefore L/D = 0.1 was designated the lower limit.

Jettison vs No Jettison

As a result of the L/D trade, an unintended trade was made to evaluate additional ways to mitigate guidance saturation at the low L/D (0.1) by adding an additional control parameter. The parameter was enabled by allowing the vehicle to jettison the HIAD in the atmosphere and transform from a lifting body to drag only. The jettison maneuver effectively fixes the apoapsis and periapsis values at the jettison point and the vehicle is able to hit the target with much higher accuracy than the no jettison case. The smaller distribution in apoapsis and periapsis altitude values is reflected in Fig. 5 and 6. It should be noted that the mechanisms that would make the jettison possible were not considered in the study.

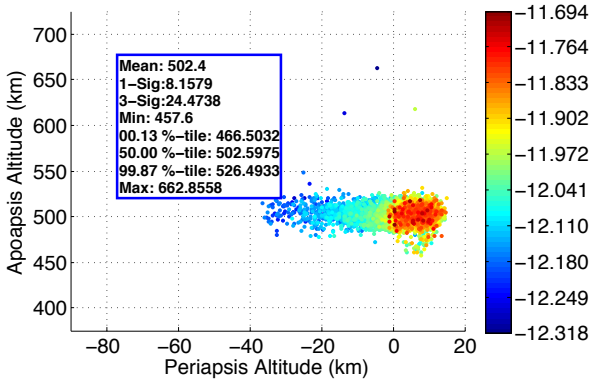

Fig. 5 L/d = 0.1, Apoapsis vs. Periapsis Altitude with Jettison

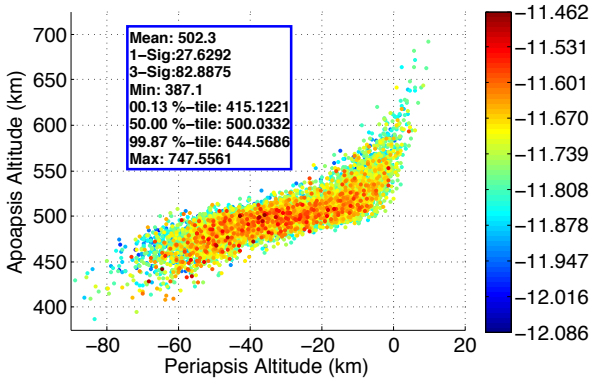

Fig. 6 L/d = 0.1, Apoapsis vs. Periapsis Altitude with no Jettison

In summary the jettison maneuver does improve the vehicle's ability to achieve a target orbit for any L/D. The necessity for the jettison maneuver becomes less critical at higher values of L/D and the decision to employ jettison for higher L/D vehicles will depend on mission specific requirements. Additionally, the modeling of the jettison maneuver is crude and factors such as HIAD separation and transitions would need to be considered if this concept were to be studied further.

500 km Circular vs 1 Sol Orbit

One final trade study was performed to determine the effect of changing the post-aerocapture target orbit for a vehicle with an L/D of 0.25. The apoapsis altitude associated with a 1 sol target orbit is 33,793 km, making it a much higher target apoapsis, requiring less energy (or ΔV) change compared to the 500 km circular orbit. The aerocapture maneuver performance is improved when more energy can be removed from

the aeropass, therefore targeting a much higher apoapsis makes executing the aerocapture maneuver more difficult. For the higher apoapsis orbits, velocity error is associated with a large error in target apoapsis altitude, which will require a larger ΔV to correct. Additionally, the lack of available corridor coupled with velocities that approach exit speeds creates the possibility of some single pass cases that do not capture into orbit. Therefore, smaller target orbits are more advantageous for aerocapture however they are more challenging for entry.

5.4 HIAD Assessment Summary

Information learned by evaluating guidances using the bank angle controller did reveal useful information for current and future studies. First, the nominal EFF aerocapture mission using a L/D of 0.25 provides sufficient targeting capability while satisfying the constraints. Second, the bank angle control was marginal (large number of trajectories saturated) for an L/D = 0.10 with no HIAD jettison. Third, jettisoning the HIAD while in the sensible atmosphere indicates a capability to improve targeting, but more analysis is required to determine if it is a viable option. Finally, CG control was demonstrated in 3DOF trajectories to be a viable option, however, the 6DOF analysis uncovered issues that require further examination. The primary issue concerns how using CG control to both control and trim the vehicle induces dynamics that may require large actuator accelerations. One recommendation is to add other CG control options to the design space, which, for example, uses the CG control for trim and an RCS system to control the induced dynamics

6. SUMMARY AND RECOMMENDATIONS

This document attempts to summarize the analysis performed to evaluate feed forward technologies in a realistic but hypothetical mission to land a 2 to 4 t power plant on Mars. The major technology recommendations that resulted from the analysis presented include: (1) need to revisit the use of rigid aeroshells based on new payload information, (2) transitions between all jettison components needs to be evaluated, (3) SRP remains on the critical path and development needs to be accelerated to a point that feasibility can be demonstrated, (3) optimize the size, shape, charring effects and CG control for HIADs, (4) consider developing a dedicated reusable testbed to test critical EDL technologies and flight instrumentation, (5) perform a aerocapture flight test, and (6) perform a flight demonstration at Mars using a useable payload using the technologies presented herein.

Much of the study effort focused on detailed subsystem model development, which uncovered many unanticipated issues. Software configuration management proved to be instrumental in allowing for rapid analysis of all aspects of the design late in the project schedule. A final recommendation is that high fidelity systems analysis can leverage work being done at many NASA centers to identify advantages and disadvantages of specific technologies considered for investment.

7. REFERENCES

1. Dwyer Cianciolo, A. M., et al. " Entry, Descent and Landing Systems Analysis Study: Phase 1 Report." NASA/TM-2010-216720.
2. Powell, R. W., Striepe, S. A., Desai, P. N., Queen, E. M., Tartabini, P. V., Brauer, G.L., Cornick, D. E., Olson, D. W., Petersen, F. M., Stevenson, R., Engle, M. C., and Marsh, S. M., "Program to Optimize Simulated Trajectories (POST2), Vol. II Utilization Manual." Version 1.1.1G, May 2000.
3. Samerah, Jamshid, "Estimating Mass of Inflatable Aerodynamic Decelerators Using Dimensionless Parameters." IPPW-8, June, 2011.
4. Dwyer Cianciolo, A. M., et al. " Entry, Descent and Landing Systems Analysis Study: Phase 2 Report on Exploration Feed-Forward Systems." NASA/TM-2011-217055.
5. Mason, L. S., "A Summary of NASA Architecture Studies Utilizing Fission Surface Power Technology," AIAA-2010-6599.
6. Samareh, J. A., and Komar, D. R., "Parametric Mass Modeling for Mars Entry, Descent and Landing System Analysis Study," AIAA-2011-1038, presented at the 49th AIAA Aerospace Sciences Meeting including the New Horizons Forum and Aerospace Exposition, Orlando, Florida, Jan. 4-7, 2011.
7. McGuire, M.K., Arnold, J. O., Covington, M.A. and Dupzyk, I. C. "Flexible Ablative Thermal Protection Sizing on Inflatable Decelerator Systems Technology for Human Mars Entry, Descent and Landing, AIAA Conference, Orlando FL, January 2011 AIAA-2011-344.
8. Beck, R. A. et al. "Overview of Initial Development of Flexible Ablators for Hypersonic Inflatable Aerodynamic Decelerators", 21st AIAA Decelerator Conference and Seminar, 23-26 May 2011,Trinity College, Dublin, Ireland.
9.Komar, D.R., Hoffman, J., and Olds, A., "Framework for the Parametric System Modeling of Space Exploration Architectures," AIAA-2008-7845, 2008.
10. Dwyer Cianciolo, A. M., et al. "Entry, Descent and Landing Systems Analysis Exploration Feed Forward Internal Peer Review Slide Package". NASA/TM-2011-217050.